

# ILP-based Local Search for Graph Partitioning

Alexandra Henzinger<sup>1</sup>, Alexander Noe<sup>2</sup>, and Christian Schulz<sup>3</sup>

- 1 Stanford University, Stanford, CA, USA  
ahenz@stanford.edu
- 2 University of Vienna, Vienna, Austria  
alexander.noe@univie.ac.at
- 3 University of Vienna, Vienna, Austria  
christian.schulz@univie.ac.at

---

## Abstract

Computing high-quality graph partitions is a challenging problem with numerous applications. In this paper, we present a novel meta-heuristic for the balanced graph partitioning problem. Our approach is based on integer linear programs that solve the partitioning problem to optimality. However, since those programs typically do not scale to large inputs, we adapt them to heuristically improve a given partition. We do so by defining a much smaller model that allows us to use symmetry breaking and other techniques that make the approach scalable. For example, in Walshaw’s well-known benchmark tables we are able to improve roughly half of all entries when the number of blocks is high.

**1998 ACM Subject Classification** G.2.2 Graph Theory

**Keywords and phrases** Graph Partitioning, Integer Linear Programming

## 1 Introduction

*Balanced graph partitioning* is an important problem in computer science and engineering with an abundant amount of application domains, such as VLSI circuit design, data mining and distributed systems [37]. It is well known that this problem is NP-complete [8] and that no approximation algorithm with a constant ratio factor exists for general graphs unless P=NP [8]. Still, there is a large amount of literature on methods (with worst-case exponential time) that solve the graph partitioning problem to optimality. This includes methods dedicated to the bipartitioning case [3, 4, 12, 13, 14, 15, 23, 21, 29, 38] and some methods that solve the general graph partitioning problem [16, 39]. Most of these methods rely on the branch-and-bound framework [27]. However, these methods can typically solve only very small problems as their running time grows exponentially, or if they can solve large bipartitioning instances using a moderate amount of time [12, 13], the running time highly depends on the bisection width of the graph. Methods that solve the general graph partitioning problem [16, 39] have huge running times for graphs with up to a few hundred vertices. Thus in practice mostly heuristic algorithms are used.

Typically the graph partitioning problem asks for a partition of a graph into  $k$  blocks of about equal size such that there are few edges between them. Here, we focus on the case when the bounds on the size are very strict, including the case of *perfect balance* when the maximal block size has to equal the average block size.

Our focus in this paper is on solution quality, i.e. minimize the number of edges that run between blocks. During the past two decades there have been numerous researchers trying to improve the best graph partitions in Walshaw’s well-known partitioning benchmark [40, 41].

Overall there have been more than forty different approaches that participated in this benchmark. Indeed, high solution quality is of major importance in applications such as VLSI Design [1, 2] where even minor improvements in the objective can have a large impact on the production costs and quality of a chip. High-quality solutions are also favorable in applications where the graph needs to be partitioned only once and then the partition is used over and over again, implying that the running time of the graph partitioning algorithms is of a minor concern [11, 18, 26, 28, 31, 30]. Thirdly, high-quality solutions are even important in areas in which the running time overhead is paramount [40], such as finite element computations [36] or the direct solution of sparse linear systems [20]. Here, high-quality graph partitions can be useful for benchmarking purposes, i.e. measuring how much more running time can be saved by higher quality solutions.

In order to compute high-quality solutions, state-of-the-art local search algorithms exchange vertices between blocks of the partition trying to decrease the cut size while also maintaining balance. This highly restricts the set of possible improvements. Recently, we introduced new techniques that relax the balance constraint for vertex movements but globally maintain balance by combining multiple local searches [35]. This was done by reducing this combination problem to finding negative cycles in a graph. In this paper, we extend the neighborhood of the combination problem by employing integer linear programming. This enables us to find even more complex combinations and hence to further improve solutions. More precisely, our approach is based on integer linear programs that solve the partitioning problem to optimality. However, out of the box those programs typically do not scale to large inputs, in particular because the graph partitioning problem has a very large amount of symmetry – given a partition of the graph, each permutation of the block IDs gives a solution having the same objective and balance. Hence, we adapt the integer linear program to improve a given input partition. We do so by defining a much smaller graph, called *model*, and solve the graph partitioning problem on the model to optimality by the integer linear program. More specifically, we select vertices close to the cut of the given input partition for potential movement and contract all remaining vertices of a block into a single vertex. A feasible partition of this model corresponds to a partition of the input graph having the same balance and objective. Moreover, this model enables us to use symmetry breaking, which allows us to scale to much larger inputs. To make the approach even faster, we combine it with initial bounds on the objective provided by the input partition, as well as providing the input partition to the integer linear program solver. Overall, we arrive at a system that is able to improve more than half of all entries in Walshaw’s benchmark when the number of blocks is high.

The rest of the paper is organized as follows. We begin in Section 2 by introducing basic concepts. After presenting some related work in Section 3 we outline the integer linear program as well as our novel local search algorithm in Section 4. Here, we start by explaining the very basic idea that allows us to find combinations of simple vertex movements. We then explain our strategies to improve the running time of the solver and strategies to select vertices for movement. A summary of extensive experiments done to evaluate the performance of our algorithms is presented in Section 5. Finally, we conclude in Section 6.

## 2 Preliminaries

### 2.1 Basic concepts

Let  $G = (V = \{0, \dots, n - 1\}, E)$  be an undirected graph. We consider positive, real-valued edge and vertex weight functions  $\omega$  resp.  $c$  and extend them to sets, i.e.,  $\omega(E') := \sum_{x \in E'} \omega(x)$

and  $c(V') := \sum_{x \in V'} c(x)$ . Let  $N(v) := \{u : \{v, u\} \in E\}$  denote the neighbors of  $v$ . The degree of a vertex  $v$  is  $d(v) := |N(v)|$ . A vertex is a *boundary vertex* if it is incident to at least one vertex in a different block. We are looking for disjoint *blocks* of vertices  $V_1, \dots, V_k$  that partition  $V$ ; i.e.,  $V_1 \cup \dots \cup V_k = V$ . The *balancing constraint* demands that each block has weight  $c(V_i) \leq (1 + \epsilon) \lceil \frac{c(V)}{k} \rceil =: L_{\max}$  for some imbalance parameter  $\epsilon$ . We call a block  $V_i$  *overloaded* if its weight exceeds  $L_{\max}$ . The objective of the problem is to minimize the total cut  $\omega(E \cap \bigcup_{i < j} V_i \times V_j)$  subject to the balancing constraints. We define the *gain* of a vertex as the maximum decrease in the cut value when moving it to a different block.

### 3 Related Work

There has been a *huge* amount of research on graph partitioning and we refer the reader to the surveys given in [6, 9, 36, 42] for most of the material. Here, we focus on issues closely related to our main contributions. All general-purpose methods that are able to obtain good partitions for large real-world graphs are based on the multi-level principle. Well-known software packages based on this approach include Jostle [42], KaHIP [33], Metis [24] and Scotch [32].

Chris Walshaw's well-known benchmark archive has been established in 2001 [40, 41]. Overall it contains 816 instances (34 graphs, 4 values of imbalance, and 6 values of  $k$ ). Ever since there have been more than forty different approaches that participated in this benchmark. In this benchmark, the running time of the participating algorithms is not measured or reported. Submitted partitions will be validated and added to the archive if they improve on a particular result. This can either be an improvement in the number of cut edges or, if they match the current best cut size, an improvement in the weight of the largest block. Most entries in the benchmark have as of Feb. 2018 been obtained by Galinier et al. [19] (more precisely an implementation of that approach by Frank Schneider), Hein and Seitzer [22] and the Karlsruhe High-Quality Graph Partitioning (KaHIP) framework [35]. More precisely, Galinier et al. [19] use a memetic algorithm that is combined with tabu search to compute solutions and Hein and Seitzer [22] solve the graph partitioning problem by providing tight relaxations of a semi-definite program into a continuous problem.

The Karlsruhe High-Quality Graph Partitioning (*KaHIP*) framework implements many different algorithms, for example flow-based methods and more-localized local searches, as well as several coarse-grained parallel and sequential meta-heuristics. KaBaPE [35] is a coarse-grained parallel evolutionary algorithm, i.e. each processor has its own population (set of partitions) and a copy of the graph. After initially creating the local population, each processor performs multi-level combine and mutation operations on the local population. This is combined with a meta-heuristic that combines local searches that individually violate the balance constraint into a more global feasible improvement. For more details, we refer the reader to [35].

### 4 Local Search based on Integer Linear Programming

We now explain our algorithm that combines integer linear programming and local search. We start by explaining the integer linear program that can solve the graph partitioning problem to optimality. However, out-of-the-box this program does not scale to large inputs, in particular because the graph partitioning problem has a very large amount of symmetry. Thus, we reduce the size of the graph by first computing a partition using an existing heuristic and based on it collapsing parts of the graph. Roughly speaking, we compute a small graph, called *model*, in which we only keep a small amount of selected vertices for

potential movement and perform graph contractions on the remaining ones. A partition of the model corresponds to a partition of the input network having the same objective and balance. The computed model is then solved to optimality using the integer linear program. As we will see this process enables us to use symmetry breaking in the linear program, which in turn drastically speeds up computation times.

#### 4.1 Integer Linear Program for the Graph Partitioning Problem

We now introduce a generalization of an integer linear program formulation for balanced bipartitioning [7] to the general graph partitioning problem. First, we introduce binary decision variables for all edges and vertices of the graph. More precisely, for each edge  $e = \{u, v\} \in E$ , we introduce the variable  $e_{uv} \in \{0, 1\}$  which is one if  $e$  is a cut edge and zero otherwise. Moreover, for each  $v \in V$  and block  $k$ , we introduce the variable  $x_{v,k} \in \{0, 1\}$  which is one if  $v$  is in block  $k$  and zero otherwise. Hence, we have a total of  $|E| + k|V|$  variables. We use the following constraints to ensure that the result is a valid  $k$ -partition:

$$\forall \{u, v\} \in E, \forall k : e_{uv} \geq x_{u,k} - x_{v,k} \quad (1)$$

$$\forall \{u, v\} \in E, \forall k : e_{uv} \geq x_{v,k} - x_{u,k} \quad (2)$$

$$\forall k : \sum_{v \in V} x_{v,k} c(v) \leq L_{\max} \quad (3)$$

$$\forall v \in V : \sum_k x_{v,k} = 1 \quad (4)$$

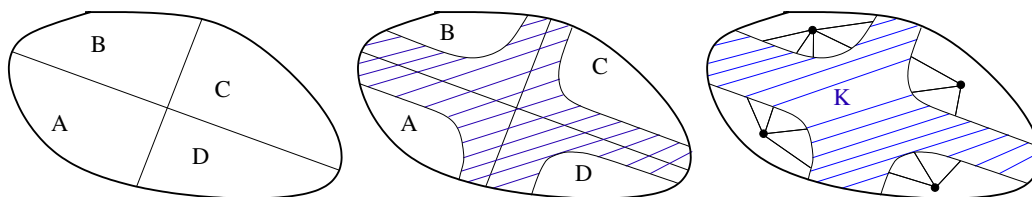
The first two constraints ensure that  $e_{uv}$  is set to one if the vertices  $u$  and  $v$  are in different blocks. For an edge  $\{u, v\} \in E$  and a block  $k$ , the right-hand side in this equation is one if one of the vertices  $u$  and  $v$  is in block  $k$  and the other one is not. If both vertices are in the same block then the right-hand side is zero for all values of  $k$ . Hence, the variable can either be zero or one in this case. However, since the variable participates in the objective function and the problem is a minimization problem, it will be zero in an optimum solution. The third constraint ensures that the balance constraint is satisfied for each partition. And finally, the last constraint ensures that each vertex is assigned to exactly one block. To sum up, our program has  $2k|E| + k + |V|$  constraints and  $k \cdot (6|E| + 2|V|)$  non-zeros. Since we want to minimize the weight of cut edges, the objective function of our program is written as:

$$\min \sum_{\{u,v\} \in E} e_{uv} \cdot \omega(\{u, v\}) \quad (5)$$

#### 4.2 Local Search

The graph partitioning problem has a large amount of symmetry – each permutation of the block IDs gives a solution with equal objective and balance. Hence, the integer linear program described above will scan many branches that contain essentially the same solutions so that the program does not scale to large instances. Moreover, it is not immediately clear how to improve the scalability of the program by using symmetry breaking or other techniques.

Our goal in this section is to develop a local search algorithm using the integer linear program above. Given a partition as input to be improved, our *main idea* is to contract vertices “that are far away” from the cut of the partition. In other words, we want to keep vertices close to the cut and contract all remaining vertices into one vertex for each block of the input partition. This ensures that a partition of the contracted graph yields a partition of the input graph with the same objective and balance. Hence, we apply the integer



■ **Figure 1** From left to right: a graph that is partitioned into four blocks, the set  $\mathcal{K}$  close to the boundary that will stay in the model, and lastly the model in which the sets  $V_i \setminus \mathcal{K}$  have been contracted.

linear program to the model and solve the partitioning problem on it to optimality. Note, however, that due to the performed contractions this does not imply an optimal solution on the input graph.

We now outline the details of the algorithm. Our local algorithm has two inputs, a graph  $G$  and a partition  $V_1, \dots, V_k$  of its vertices. For now assume that we have a set of vertices  $\mathcal{K} \subset V$  which we want to keep in the coarse model, i.e. a set of vertices which we do not want to contract. We outline in Section 4.4 which strategies we have to select the vertices  $\mathcal{K}$ . For the purpose of contraction we define  $k$  sets  $\mathcal{V}_i := V_i \setminus \mathcal{K}$ . We obtain our coarse model by contracting each of these vertex sets. The contraction of a vertex set  $\mathcal{V}_i$  works as follows: the set of vertices is contracted into a single vertex  $\mu_i$ . The weight of  $\mu_i$  is set to the sum of the weight of all vertices in the set that is contracted. There is an edge between two vertices  $\mu_i$  and  $v$  in the contracted graph if there is an edge between a vertex of the set and  $v$  in the original graph  $G$ . The weight of an edge  $(\mu_i, v)$  is set to the sum of the weight of edges that run between the vertices of the set and  $v$ . After all contractions have been performed the coarse model contains  $k + |\mathcal{K}|$  vertices, and potentially much less edges than the input graph. Figure 1 gives an abstract example of our model.

There are two things that are important to see: first, due to the way we perform contraction, the given partition of the input network yields a partition of our coarse model that has the same objective and balance simply by putting  $\mu_i$  into block  $i$  and keeping the block of the input for the vertices in  $\mathcal{K}$ . Moreover, if we compute a new partition of our coarse model, we can build a partition in the original graph with the same properties by putting the vertices  $\mathcal{V}_i$  into the block of their coarse representative  $\mu_i$  together with the vertices of  $\mathcal{K}$  that are in this block. Hence, we can solve the integer linear program on the coarse model to compute a partition for the input graph. After the solver terminates, i.e. found an optimum solution of our mode or has reached a predefined time limit  $\mathcal{T}$ , we transfer the best solution to the original graph. Note that the latter is possible since an integer linear program solver typically computes intermediate solutions that may not be optimal.

### 4.3 Optimizations

Independent of the vertices  $\mathcal{K}$  that are selected to be kept in the coarse model, the approach above allows us to define optimizations to solve our integer linear program faster. We apply four strategies: (i) symmetry breaking, (ii) providing a start solution to the solver, (iii) add the objective of the input as a constraint as well as (iv) using the parallel solving facilities of the underlying solver. We outline the first three strategies in greater detail:

**Symmetry Breaking.** If the set  $\mathcal{K}$  is small, then the solver will find a solution much faster. Ideally, our algorithms selects the vertices  $\mathcal{K}$  such that  $c(\mu_i) + c(\mu_j) > L_{\max}$ . In other words,

no two contracted vertices can be clustered in one block. We can use this to break symmetry in our integer linear programming by adding constraints that fix the block of  $\mu_i$  to block  $i$ , i.e. we set  $x_{\mu_i,i} = 1$  and  $x_{\mu_i,j} = 0$  for  $i \neq j$ . Moreover, for those vertices we can remove the constraint which ensures that the vertex is assigned to a single unique block—since we assigned those vertices to a block using the new additional constraints.

**Providing a Start Solution to the Solver.** The integer linear program performs a significant amount of work in branches which correspond to solutions that are worse than the input partitioning. Only very few - if any - solutions are better than the given partition. However, we already know a fairly good partition (the given partition from the input) and give this partition to the solver by setting according initial values for all variables. This ensures that the integer linear program solver can omit many branches and hence speeds up the time needed to solve the integer linear program.

**Solution Quality as a Constraint.** Since we are only interested in improved partitions, we can add an additional constraint that disallows solutions which have a worse objective than the input partition. Indeed, the objective function of the linear program is linear, and hence the additional constraint is also linear. Depending on the objective value, this reduces the number of branches that the linear program solver needs to look at. However, note that this comes at the cost of an additional constraint that needs to be evaluated.

#### 4.4 Vertex Selection Strategies

The algorithm above works for different vertex sets  $\mathcal{K}$  that should be kept in the coarse model. There is an obvious trade-off: on the one hand, the set  $\mathcal{K}$  should not be too large, otherwise the coarse model would be large and hence the linear programming solver needs a large amount of time to find a solution. On the other hand, the set should also not be too small, since this restricts the amount of possible vertex movements, and hence the approach is unlikely to find an improved solution. We now explain different strategies to select the vertex set  $\mathcal{K}$ . In any case, while we add vertices to the set  $\mathcal{K}$ , we compute the number of non-zeros in the corresponding ILP. We stop to add vertices when the number of non-zeros in the corresponding ILP is larger than a parameter  $\mathcal{N}$ .

**Vertices Close to Input Cut.** The intuition of the first strategy, **Boundary**, is that changes or improvements of the partition will occur reasonable close to the input partition. In this simple strategy our algorithm tries to use all *boundary vertices* as the set  $\mathcal{K}$ . In order to adhere to the constraint on the number of non-zeros in the ILP, we add the vertices of the boundary uniformly at random and stop if the number of non-zeros  $\mathcal{N}$  is reached. If the algorithm managed to add all boundary vertices whilst not exceeding the specified number of non-zeros, we do the following extension: we perform a breadth-first search that is initialized with a random permutation of the boundary vertices. All additional vertices that are reached by the BFS are added to  $\mathcal{K}$ . As soon as the number of non-zeros  $\mathcal{N}$  is reached, the algorithm stops.

**Start at Promising Vertices.** Especially for high values of  $k$  the boundary contains many vertices. The **Boundary** strategy quickly adds a lot of random vertices while ignoring vertices that have high gain. However, note that even in good partitions it is possible that vertices with positive gain exist but cannot be moved due to the balance constraint.

Hence, our second strategy,  $\text{Gain}_\rho$ , tries to fix this issue by starting a breadth-first search initialized with only high gain vertices. More precisely, we initialize the BFS with each vertex having gain  $\geq \rho$  where  $\rho$  is a tuning parameter. Our last strategy,  $\text{TopVertices}_\delta$ , starts by sorting the boundary vertices by their gain. We break ties uniformly at random. Vertices are then traversed in decreasing order (highest gain vertices first) and for each start vertex  $v$  our algorithm adds all vertices with distance  $\leq \delta$  to the model. The algorithm stops as soon as the number of non-zeros exceeds  $\mathcal{N}$ .

Early gain-based local search heuristics for the  $\epsilon$ -balanced graph partitioning problem searched for pairwise swaps with positive gain [17, 25]. More recent algorithms generalized this idea to also search for cycles or paths with positive total gain [35]. An important advantage of our new approach is that we solve the combination problem to optimality, i.e. our algorithm finds the best combination of vertex movements of the vertices in  $\mathcal{K}$  w.r.t to the input partition of the original graph. Therefore we can also find more complex optimizations that cannot be reduced to positive gain cycles and paths.

## 5 Experiments

### 5.1 Experimental Setup and Methodology

We implemented the algorithms using C++-17 and compiled all codes using g++-7.2.0 with full optimization (-O3). We use Gurobi 7.5.2 as an ILP solver and always use its parallel version. We perform experiments on the Phase 2 Haswell nodes of the SuperMUC supercomputer. The Phase 2 of SuperMUC consists of 3072 nodes, each with two Haswell Xeon E5-2697 v3 processors. Each node has 28 cores at 2.6GHz, as well as 64GB of main memory and runs the SUSE Linux Enterprise Server (SLES) operating system. Unless otherwise mentioned, our approach uses the shared-memory parallel variant of Gurobi using all 28 cores of a single node of the machine. In general, we perform five repetitions per instance and report the average running time as well as cut. Unless otherwise mentioned, we use a time limit for the integer linear program. When the time limit is passed, the integer linear program solver outputs the best solution that has currently been discovered. This solution does not have to be optimal. Note that we do not perform experiments with Metis [24] and Scotch [32] in here, since previous papers, e.g. [33, 34], have already shown that solution quality obtained is much worse than results achieved in the Walshaw benchmark. When averaging over multiple instances, we use the geometric mean in order to give every instance the same influence on the *final score*.

**Performance Plots.** These plots relate the fastest running time to the running time of each other ILP-based local search algorithm on a per-instance basis. For each algorithm, these ratios are sorted in increasing order. The plots show the ratio  $t_{\text{best}}/t_{\text{algorithm}}$  on the y-axis to highlight the instances in which each algorithm performs badly. For plots in which we measure solution quality, the y-axis shows the ratio  $\text{cut}_{\text{best}}/\text{cut}_{\text{algorithm}}$ . A point close to zero indicates that the running time/quality of the algorithm was considerably worse than the fastest/best algorithm on the same instance. A value of one therefore indicates that the corresponding algorithm was one of the fastest/best algorithms to compute the solution. Thus an algorithm is considered to outperform another algorithm if its corresponding ratio values are above those of the other algorithm. In order to include instances that hit the time limit, we set the corresponding values below *zero* for ratio computations.

■ **Table 1** Basic properties of the our benchmark instances.

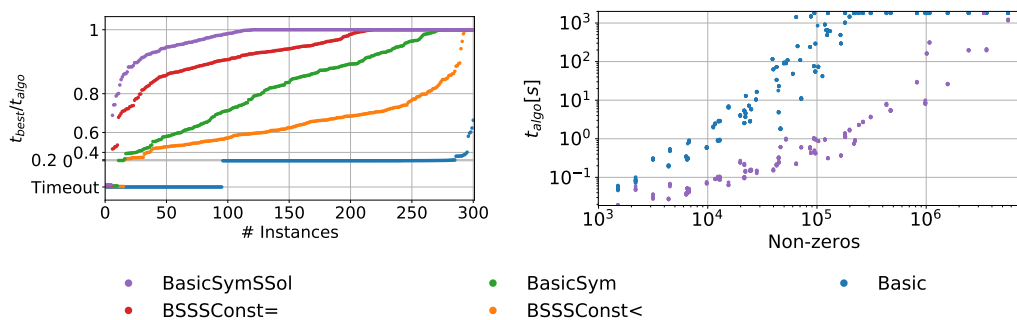
Graph	$n$	$m$	Graph	$n$	$m$
Walshaw Graphs (Set B)			Walshaw Graphs (Set B)		
add20	2 395	7 462	wing	62 032	$\approx$ 121K
data	2 851	15 093	brack2	62 631	$\approx$ 366K
3elt	4 720	13 722	finan512	74 752	$\approx$ 261K
uk	4 824	6 837	fe_tooth	78 136	$\approx$ 452K
add32	4 960	9 462	fe_rotor	99 617	$\approx$ 662K
bcsstk33	8 738	$\approx$ 291K	598a	110 971	$\approx$ 741K
whitaker3	9 800	28 989	fe_ocean	143 437	$\approx$ 409K
crack	10 240	30 380	144	144 649	$\approx$ 1.1M
wing_nodal	10 937	75 488	wave	156 317	$\approx$ 1.1M
fe_4elt2	11 143	32 818	m14b	214 765	$\approx$ 1.7M
vibrobox	12 328	$\approx$ 165K	auto	448 695	$\approx$ 3.3M
bcsstk29	13 992	$\approx$ 302K	Parameter Tuning (Set A)		
4elt	15 606	45 878	delaunay_n15	32 768	98 274
fe_sphere	16 386	49 152	rgg_15	32 768	$\approx$ 160K
cti	16 840	48 232	2cubes_sphere	101 492	$\approx$ 772K
memplus	17 758	54 196	cf2	123 440	$\approx$ 1.5M
cs4	22 499	43 858	boneS01	127 224	$\approx$ 3.3M
bcsstk30	28 924	$\approx$ 1.0M	Dubcova3	146 689	$\approx$ 1.7M
bcsstk31	35 588	$\approx$ 572K	G2_circuit	150 102	$\approx$ 288K
fe_pwt	36 519	$\approx$ 144K	thermal2	1 227 087	$\approx$ 3.7M
bcsstk32	44 609	$\approx$ 985K	as365	3 799 275	$\approx$ 11.4M
fe_body	45 087	$\approx$ 163K	adaptive	6 815 744	$\approx$ 13.6M
t60k	60 005	89 440			

**Instances.** We perform experiments on two sets of instances. Set  $A$  is used to determine the performance of the integer linear programming optimizations and to tune the algorithm. We obtained these instances from the Florida Sparse Matrix collection [10] and the 10th DIMACS Implementation Challenge [5] to test our algorithm. Set  $B$  are all graphs from Chris Walshaw’s graph partitioning benchmark archive [40, 41]. This archive is a collection of instances from finite-element applications, VLSI design and is one of the default benchmarking sets for graph partitioning.

Table 1 gives basic properties of the graphs from both benchmark sets. We ran the unoptimized integer linear program that solves the graph partitioning problem to optimality from Section 4.1 on the five smallest instances from the Walshaw benchmark set. With a time limit of 30 minutes, the solver has only been able to compute a solution for two graphs with  $k = 2$ . For higher values of  $k$  the solver was unable to find any solution in the time limit. Even applying feasible optimizations does not increase the amount of ILPs solved. Hence, we omit further experiments in which we run an ILP solver on the full graph.

## 5.2 Impact of Optimizations

We now evaluate the impact of the optimization strategies for the ILP that we presented in Section 4.3. In this section, we use the variant of our local search algorithm in which  $\mathcal{K}$  is obtained by starting depth-one breadth-first search at the 25 highest gain vertices, and set the limit on the non-zeros in the ILP to  $\mathcal{N} = \infty$ . However, we expect the results in terms of speedup to be similar for different vertex selection strategies. To evaluate the ILP performance, we run KaFFPa using the strong preconfiguration on each of the graphs from



■ **Figure 2** *Left*: performance plot for five variants of our algorithm: **Basic** does not contain any optimizations; **BasicSym** enables symmetry breaking; **BasicSymSSol** additionally gives the input partitioning to the ILP solver. The two variants **BSSSSConst=** and **BSSSSConst<** are the same as **BasicSymSSol** with additional constraints: **BSSSSConst=** has the additional constraint that the objective has to be smaller or equal to the start solution, **BSSSSConst<** has the constraint that the solution must be better than the start solution. *Right*: performance of the slowest (**Basic**) and fastest ILPs (**BasicSymSSol**) depending on the number of non-zeros in the ILP.

set  $A$  using  $\epsilon = 0$  and  $k \in \{2, 4, 8, 16, 32, 64\}$  and then use the computed partition as input to each ILP (with the different optimizations). As the optimizations do not change the objective value achieved in the ILP, we only report running times of our different approaches. We set the time limit of the ILP solver to 30 minutes.

We use five variants of our algorithm: **Basic** does not contain any optimizations; **BasicSym** enables symmetry breaking; **BasicSymSSol** additionally gives the input partitioning to the ILP solver. The two variants **BSSSSConst=** and **BSSSSConst<** are the same as **BasicSymSSol** with additional constraints: **BSSSSConst=** has the additional constraint that the objective has to be smaller or equal to the start solution, **BSSSSConst<** has the constraint that the objective value of a solution must be better than the objective value of the start solution. Figure 3 summarises the results.

In our experiments, the basic configuration reaches the time limit in 95 out of the 300 runs. Overall, enabling symmetry breaking drastically speeds up computations. On all of the instances which the **Basic** configuration could solve within the time limit, each other configuration is faster than the **Basic** configuration. Symmetry breaking speeds up computations by a factor of 41 in the geometric mean on those instances. The largest obtained speedup on those instances was a factor of 5663 on the graph adaptive for  $k = 32$ . The configuration solves all but the two instances (boneS01,  $k = 32$ ) and (Dubcova3,  $k = 16$ ) within the time limit. Additionally providing the start solution (**BasicSymSSol**) gives an addition speedup of 22% on average. Over the **Basic** configuration, the average speedup is 50 with the largest speedup being 6495 and the smallest speedup being 47%. This configuration can solve all instances within the time limit except the instance boneS01 for  $k = 32$ . Providing the objective function as a constraint (or strictly smaller constraint) does not further reduce the running time of the solver. Instead, the additional constraints even increase the running time. We adhere this to the fact that the solver has to do additional work to evaluate the constraint. We conclude that **BasicSymSSol** is the fastest configuration of the ILP. Hence, we use this configuration in all the following experiments. Moreover, from Figure 2 we can see that this configuration can solve most of the instance within the time limit if the number of non-zeros in the ILP is below  $10^6$ . Hence, we set the parameter  $\mathcal{N}$  to  $10^6$  in the following section.

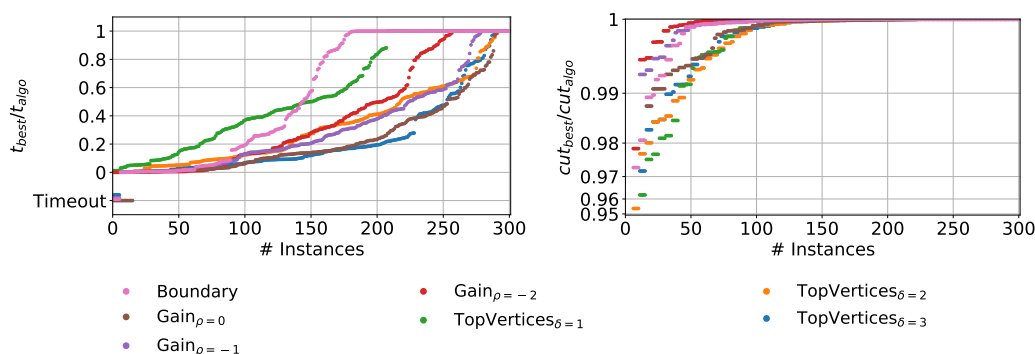
### 5.3 Vertex Selection Rules

We now evaluate the vertex selection strategies to find the set of vertices  $\mathcal{K}$  that model the ILP. We look at all strategies described in Section 4.4, i.e. **Boundary**, **Gain** $_{\rho}$  with the parameter  $\rho \in \{-2, -1, 0, 1\}$  as well as **TopVertices** $_{\delta}$  for  $\delta \in \{1, 2, 3\}$ . To evaluate the different selection strategies, we use the best of five runs of KaFFPa, strong on each of the graphs from set  $A$  using  $\epsilon = 0$  and  $k \in \{2, 4, 8, 16, 32, 64\}$  and then use the computed partition as input to the ILP (with different sets  $\mathcal{K}$ ). Table 2 summarizes the results of the experiment, i.e. the number of cases in which our algorithm was able to improve the result, the average running time in seconds for these selection strategies as well as the number of cases in which the strategy computed the best result (the partition having the lowest cut). We set the time limit to 2 days to be able to finish almost all runs without running into timeout. For the average running time we exclude all graphs in which at least one algorithm did not finish in 2 days (rgg\_15  $k = 16$ , delaunay\_n15  $k = 4$ , G2\_circuit  $k = 4, 8$ ). If multiple runs share the best result, they are all counted. However, when no algorithm improves the input partition on a graph, we do not count them.

Looking at the number of improvements, the **Boundary** strategy is able to improve the input for small values of  $k$ , but with increasing number of blocks  $k$  improvements decrease to no improvement in all runs with  $k = 64$ . Because of the limit on the number of non-zeros, the ILP contains only random boundary vertices for large values of  $k$  in this case. Hence, there are not sufficiently many high gain vertices in the model and fewer improvements for large values of  $k$  are expected. For small values of  $k \in \{2, 4\}$ , the **Boundary** strategy can

■ **Table 2** From top to bottom: Number of improvements found by different vertex selection rules relative to the total number of instances, average running time of the strategy on the subset of instances (graph,  $k$ ) in which all strategies finished within the time limit, and the relative number of instances in which the strategy computed the lowest cut. Best values are highlighted in bold.

$k$	Gain			TopVertices			Boundary
	$\rho = 0$	$\rho = -1$	$\rho = -2$	$\delta = 1$	$\delta = 2$	$\delta = 3$	
	Relative Number of Improvements						
2	<b>70%</b>	<b>70%</b>	<b>70%</b>	50%	<b>70%</b>	<b>70%</b>	<b>70%</b>
4	50%	60%	<b>80%</b>	70%	70%	70%	<b>80%</b>
8	50%	60%	<b>78%</b>	60%	60%	60%	48%
16	30%	50%	<b>70%</b>	40%	30%	30%	40%
32	<b>60%</b>	<b>60%</b>	46%	50%	50%	20%	20%
64	<b>70%</b>	<b>70%</b>	50%	30%	20%	20%	0%
	Average Running Time						
2	189.943s	292.573s	357.145s	<b>34.045s</b>	61.152s	92.452s	684.198s
4	996.934s	628.950s	428.353s	<b>87.357s</b>	255.223s	558.578s	1467.595s
8	552.183s	244.470s	244.046s	105.737s	167.164s	340.900s	<b>96.763s</b>
16	118.532s	52.547s	90.363s	53.385s	141.814s	243.957s	<b>34.790s</b>
32	40.300s	24.607s	94.146s	27.156s	80.252s	116.023s	<b>7.596s</b>
64	15.866s	21.908s	24.253s	14.627s	30.558s	44.813s	<b>4.187s</b>
	Relative Number Best Algorithm						
2	20%	<b>60%</b>	50%	10%	10%	0%	<b>60%</b>
4	10%	0%	<b>50%</b>	10%	0%	0%	30%
8	0%	20%	<b>30%</b>	10%	10%	10%	26%
16	0%	10%	<b>54%</b>	10%	0%	10%	20%
32	0%	8%	<b>38%</b>	0%	0%	0%	4%
64	0%	16%	<b>36%</b>	0%	0%	0%	0%



■ **Figure 3** *Left*: performance plot for all vertex selection strategies *Right*: cut value of vertex selection strategies in comparison to the best result given by any strategy.

improve as many as the  $\text{Gain}_{\rho=-2}$  strategy but the average running times are higher.

For  $k = \{2, 4, 8, 16\}$ , the strategy  $\text{Gain}_{\rho=-2}$  has the highest number of improvements, for  $k = \{32, 64\}$  it is surpassed by the strategy  $\text{Gain}_{\rho=-1}$ . However, the strategy  $\text{Gain}_{\rho=-2}$  finds the best cuts in most cases among all tested strategies. Due to the way these strategies are designed, they are able to put a lot of high gain vertices into the model as well as vertices that can be used to balance vertex movements. The  $\text{TopVertices}$  strategies are overall also able to find a large number of improvements. However, the found improvements are typically smaller than the  $\text{Gain}$  strategies. This is due to the fact that the  $\text{TopVertices}$  strategies grow BFS balls with a predefined depth around high gain vertices first, and later on are not able to include vertices that could be used to balance their movement. Hence, there are less potential vertex movements that could yield an improvement.

For almost all strategies, we can see that the average running time decreases as the number of blocks  $k$  increases. This happens because we limit the number of non-zeros  $\mathcal{N}$  in our ILP. As the number of non-zeros grows linear with the underlying model size, the models are far smaller for higher values of  $k$ . Using symmetry breaking, we already fixed the block of the  $k$  vertices  $\mu_i$  which represent the vertices not part of  $\mathcal{K}$ . Thus the ILP solver can quickly prune branches which would place vertices connected heavily to one of these vertices in a different block. Additionally, our data indicate that a large number of small areas in our model results faster in solve times than when the model contains few large areas. The performance plot in Figure 3 shows that the strategies  $\text{Boundary}$ ,  $\text{TopVertices}_{\delta=1}$  and  $\text{Gain}_{\rho=-2}$  have lower running times than other strategies. These strategies all select a large number of vertices to initialize the breadth-first search. Therefore they output a vertex set  $\mathcal{K}$  that is the union of many small areas around these vertices. Variants that initialize the breadth-first search with fewer vertices have fewer areas, however each of the areas is larger.

## 5.4 Walshaw Benchmark

In this section, we present the results when running our best configuration on all graphs from Walshaw’s benchmark archive. Note that the rules of the benchmark imply that running time is not an issue, but algorithms should achieve the smallest possible cut value while satisfying the balance constraint. We run our algorithm in the following setting: We take existing partitions from the archive and use those as input to our algorithm. As indicated by the experiments in Section 5.3, the vertex selection strategies  $\text{Gain}_{\rho \in \{-1, -2\}}$  perform best for different values of  $k$ . Thus we use the variant  $\text{Gain}_{\rho=-2}$  for  $k \leq 16$  and both  $\text{Gain}_{\rho=-2}$  and  $\text{Gain}_{\rho=-1}$  otherwise in this section. We repeat the experiment once for each

instance (graph,  $k$ ) and run our algorithm for  $k = \{2, 4, 8, 16, 32, 64\}$  and  $\epsilon \in \{0, 1\%, 3\%, 5\%\}$ . For larger values of  $k \in \{32, 64\}$ , we strengthen our strategy and use  $\mathcal{N} = 5 \cdot 10^6$  as a bound for the number of non-zeros. Table 3 summarizes the results and Table 7 in the Appendix gives detailed per-instance results.

When running our algorithm using the currently best partitions provided in the benchmark, we are able to improve 38% of the currently reported perfectly balanced results. We are able to improve a larger amount of results for larger values of  $k$ , more specifically, out of the partitions with  $k \geq 16$ , we can improve 60% of all perfectly balanced partitions. This is due to the fact that the graph partitioning problem becomes more difficult for larger values of  $k$ . There is a wide range of improvements with the smallest improvement being 0.0008% for graph auto with  $k = 32$  and  $\epsilon = 3\%$  and with the largest improvement that we found being 1.72% for fe\_body for  $k = 32$  and  $\epsilon = 0\%$ . The largest absolute improvement we found is 117 for bcsstk32 with  $k = 64$  and  $\epsilon = 0\%$ . In general, the total number of improvements becomes less if more imbalance is allowed. This is also expected since traditional local search methods have a larger amount of freedom to move vertices. However, the number of improvements still shows that the method is also able to improve a large number of partitions for large values of  $k$  even if more imbalance is allowed.

■ **Table 3** Relative number of improved instances in the Walshaw Benchmark starting from current entries reported in the Walshaw benchmark.

$k/\epsilon$	0%	1%	3%	5%
2	6%	12%	6%	6%
4	18%	9%	6%	18%
8	26%	24%	12%	15%
16	50%	26%	29%	29%
32	62%	47%	47%	53%
64	68%	59%	71%	76%
sum	38%	29%	28%	33%

## 6 Conclusions and Future Work

We presented a novel meta-heuristic for the balanced graph partitioning problem. Our approach is based on an integer linear program that solves a model to combine unconstrained vertex movements into a global feasible improvement. Through a given input partition, we were able to use symmetry breaking and other techniques that make the approach scale to large inputs. In Walshaw’s well known benchmark tables, we were able to improve a large amount of partitions given in the benchmark.

In the future, we plan to further improve our implementation and integrate it into the KaHIP framework. We would like to look at other objective functions as long as they can be modelled linearly. Moreover, we want to investigate whether this kind of contractions can be useful for other ILPs. It may be interesting to find cores for contraction by using the information provided an evolutionary algorithm like KaFFPaE [34], i.e. if many of the individuals of the population of the evolutionary algorithm agree that two vertices should be put together in a block then those should be contracted in our model. Lastly, besides using other exact techniques like branch-and-bound to solve our combination model, it may also be worthwhile to use a heuristic algorithm instead.

## Acknowledgements

The research leading to these results has received funding from the European Research Council under the European Community’s Seventh Framework Programme (FP7/2007-2013)/ERC grant agreement No. 340506. Moreover, the authors gratefully acknowledge the Gauss Centre for Supercomputing e.V. ([www.gauss-centre.eu](http://www.gauss-centre.eu)) for funding this project by providing computing time on the GCS Supercomputer SuperMUC at Leibniz Supercomputing Centre ([www.lrz.de](http://www.lrz.de)).

---

**References**

---

- 1 C. J. Alpert and A. B. Kahng. Recent Directions in Netlist Partitioning: A Survey. *Integration, the VLSI Journal*, 19(1-2):1–81, 1995.
- 2 C. J. Alpert, A. B. Kahng, and S. Z. Yao. Spectral Partitioning with Multiple Eigenvectors. *Discrete Applied Mathematics*, 90(1):3–26, 1999.
- 3 M. Armbruster. *Branch-and-Cut for a Semidefinite Relaxation of Large-Scale Minimum Bisection Problems*. PhD thesis, 2007.
- 4 M. Armbruster, M. Fügenschuh, C. Helmberg, and A. Martin. A Comparative Study of Linear and Semidefinite Branch-and-Cut Methods for Solving the Minimum Graph Bisection Problem. In *Proc. of the 13th International Conference on Integer Programming and Combinatorial Optimization*, volume 5035 of *LNCS*, pages 112–124. Springer, 2008.
- 5 D. A. Bader, H. Meyerhenke, P. Sanders, C. Schulz, A. Kappes, and D. Wagner. Benchmarking for Graph Clustering and Partitioning. In *Encyclopedia of Social Network Analysis and Mining*, pages 73–82. Springer, 2014.
- 6 C. Bichot and P. Siarry, editors. *Graph Partitioning*. Wiley, 2011.
- 7 R. Brillout. A Multi-Level Framework for Bisection Heuristics. 2009.
- 8 T. N. Bui and C. Jones. Finding Good Approximate Vertex and Edge Partitions is NP-Hard. *Information Processing Letters*, 42(3):153–159, 1992.
- 9 A. Buluç, H. Meyerhenke, I. Safro, P. Sanders, and C. Schulz. Recent Advances in Graph Partitioning. In *Algorithm Engineering*, pages 117–158. Springer, 2016.
- 10 T. Davis. The University of Florida Sparse Matrix Collection.
- 11 D. Delling, A. V. Goldberg, T. Pajor, and R. F. Werneck. Customizable Route Planning. In *Proc. of the 10th International Symposium on Experimental Algorithms*, volume 6630 of *LCNS*, pages 376–387. Springer, 2011.
- 12 D. Delling, A. V. Goldberg, I. Razenshteyn, and R. F. Werneck. Exact Combinatorial Branch-and-Bound for Graph Bisection. In *Proc. of the 12th Workshop on Algorithm Engineering and Experimentation (ALENEX'12)*, pages 30–44, 2012.
- 13 D. Delling and R. F. Werneck. Better Bounds for Graph Bisection. In *Proc. of the 20th European Symposium on Algorithms*, volume 7501 of *LNCS*, pages 407–418, 2012.
- 14 A. Feldmann and P. Widmayer. An  $O(n^4)$  Time Algorithm to Compute the Bisection Width of Solid Grid Graphs. In *Proc. of the 19th European Conference on Algorithms*, volume 6942 of *LNCS*, pages 143–154. Springer, 2011.
- 15 A. Felner. Finding Optimal Solutions to the Graph Partitioning Problem with Heuristic Search. *Annals of Mathematics and Artificial Intelligence*, 45:293–322, 2005.
- 16 C. E. Ferreira, A. Martin, C. C. De Souza, R. Weismantel, and L. A. Wolsey. The Node Capacitated Graph Partitioning Problem: A Computational Study. *Mathematical Programming*, 81(2):229–256, 1998.
- 17 C. M. Fiduccia and R. M. Mattheyses. A Linear-Time Heuristic for Improving Network Partitions. In *Proc. of the 19th Conference on Design Automation*, pages 175–181, 1982.
- 18 J. Fietz, M. Krause, C. Schulz, P. Sanders, and V. Heuveline. Optimized Hybrid Parallel Lattice Boltzmann Fluid Flow Simulations on Complex Geometries. In *Proc. of Euro-Par 2012 Parallel Processing*, volume 7484 of *LNCS*, pages 818–829. Springer, 2012.
- 19 P. Galinier, Z. Boujbel, and M. C. Fernandes. An Efficient Memetic Algorithm for the Graph Partitioning Problem. *Annals of Operations Research*, 191(1):1–22, 2011.
- 20 A. George. Nested Dissection of a Regular Finite Element Mesh. *SIAM Journal on Numerical Analysis*, 10(2):345–363, 1973.
- 21 W. W. Hager, D. T. Phan, and H. Zhang. An Exact Algorithm for Graph Partitioning. *Mathematical Programming*, 137(1-2):531–556, 2013.
- 22 M. Hein and S. Setzer. Beyond Spectral Clustering - Tight Relaxations of Balanced Graph Cuts. In *Advances in Neural Information Processing Systems*, pages 2366–2374, 2011.

- 23 S. E. Karisch, F. Rendl, and J. Clausen. Solving Graph Bisection Problems with Semidefinite Programming. *INFORMS Journal on Computing*, 12(3):177–191, 2000.
- 24 G. Karypis and V. Kumar. A Fast and High Quality Multilevel Scheme for Partitioning Irregular Graphs. *SIAM Journal on Scientific Computing*, 20(1):359–392, 1998.
- 25 B. W. Kernighan and S. Lin. An Efficient Heuristic Procedure for Partitioning Graphs. *The Bell System Technical Journal*, 49(1):291–307, 1970.
- 26 T. Kieritz, D. Luxen, P. Sanders, and C. Vetter. Distributed Time-Dependent Contraction Hierarchies. In *Proc. of the 9th International Symposium on Experimental Algorithms*, volume 6049 of *LNCS*, pages 83–93. Springer, 2010.
- 27 A. H. Land and A. G. Doig. An Automatic Method of Solving Discrete Programming Problems. *Econometrica*, 28(3):497–520, 1960.
- 28 U. Lauther. An Extremely Fast, Exact Algorithm for Finding Shortest Paths in Static Networks with Geographical Background, 2004.
- 29 A. Lisser and F. Rendl. Graph Partitioning using Linear and Semidefinite Programming. *Mathematical Programming*, 95(1):91–101, 2003. doi:10.1007/s10107-002-0342-x.
- 30 D. Luxen and D. Schieferdecker. Candidate Sets for Alternative Routes in Road Networks. In *Proc. of the 11th International Symposium on Experimental Algorithms (SEA'12)*, volume 7276 of *LNCS*, pages 260–270. Springer, 2012.
- 31 R. H. Möhring, H. Schilling, B. Schütz, D. Wagner, and T. Willhalm. Partitioning Graphs to Speedup Dijkstra’s Algorithm. *Journal of Experimental Algorithmics (JEA)*, 11(2006), 2007.
- 32 F. Pellegrini. Scotch Home Page. <http://www.labri.fr/pelegrin/scotch>.
- 33 P. Sanders and C. Schulz. Engineering Multilevel Graph Partitioning Algorithms. In *Proc. of the 19th European Symp. on Algorithms*, volume 6942 of *LNCS*, pages 469–480. Springer, 2011.
- 34 P. Sanders and C. Schulz. Distributed Evolutionary Graph Partitioning. In *Proc. of the 12th Workshop on Algorithm Engineering and Experimentation (ALENEX'12)*, pages 16–29, 2012.
- 35 P. Sanders and C. Schulz. Think Locally, Act Globally: Highly Balanced Graph Partitioning. In *Proc. of the 12th Int. Symp. on Experimental Algorithms (SEA'13)*, LNCS. Springer, 2013.
- 36 K. Schloegel, G. Karypis, and V. Kumar. Graph Partitioning for High Performance Scientific Simulations. In *The Sourcebook of Parallel Computing*, pages 491–541, 2003.
- 37 C. Schulz and D. Strash. Graph Partitioning Formulations and Applications to Big Data. In *Encyclopedia on Big Data Technologies*, 2018, to appear.
- 38 M. Sellmann, N. Sensen, and L. Timajev. Multicommodity Flow Approximation used for Exact Graph Partitioning. In *Proc. of the 11th European Symposium on Algorithms*, volume 2832 of *LNCS*, pages 752–764. Springer, 2003.
- 39 N. Sensen. Lower Bounds and Exact Algorithms for the Graph Partitioning Problem Using Multicommodity Flows. In *Proc. of the 9th European Symposium on Algorithms*, volume 2161 of *LNCS*, pages 391–403. Springer, 2001.
- 40 A. J. Soper, C. Walshaw, and M. Cross. A Combined Evolutionary Search and Multilevel Optimisation Approach to Graph-Partitioning. *Journal of Global Optimization*, 29(2):225–241, 2004.
- 41 C. Walshaw. Walshaw Partitioning Benchmark. <http://staffweb.cms.gre.ac.uk/~wc06/partition/>.
- 42 C. Walshaw and M. Cross. JOSTLE: Parallel Multilevel Graph-Partitioning Software – An Overview. In *Mesh Partitioning Techniques and Domain Decomposition Techniques*, pages 27–58. 2007.

## A Additional Tables

■ **Table 4** Improvement of existing partitions from the Walshaw benchmark with  $\epsilon = 0\%$  using our ILP approach. In each  $k$ -column the results computed by our approach are on the left and the current Walshaw cuts are on the right. Results achieved by  $\text{Gain}_{\rho=-1}$  are marked with  $\hat{\phantom{x}}$  and results achieved by  $\text{Gain}_{\rho=-2}$  are marked with  $*\phantom{x}$ .

Graph / k	2		4		8		16		32		64	
add20	596	596	1151	1151	1681	1681	2040	2040	<b>*2360</b>	2361	$\hat{\phantom{x}}2947$	2949
data	189	189	382	382	668	668	1127	1127	1799	1799	2839	2839
3elt	90	90	201	201	345	345	573	573	960	960	1532	1532
uk	19	19	41	41	83	83	145	145	<b>*246</b>	247	408	408
add32	11	11	34	34	67	67	118	118	213	213	485	485
bcstkt33	10171	10171	21717	21717	34437	34437	54680	54680	77414	77414	107185	107185
whitaker3	127	127	381	381	656	656	1085	1085	1668	1668	2491	2491
crack	184	184	366	366	679	679	1088	1088	<b>*1678</b>	1679	2535	2535
wing_nodal	1707	1707	3575	3575	5435	5435	<b>*8333</b>	8334	11768	11768	<b>*15774</b>	15775
fe_4elt2	130	130	349	349	607	607	1007	1007	1614	1614	2475	2478
vibrobox	10343	10343	18976	18976	24484	24484	<b>*31848</b>	31850	<b>*39474</b>	39477	<b>*46568</b>	46571
bcstkt29	2843	2843	8035	8035	13975	13975	21905	21905	<b>*34733</b>	34737	55241	55241
4elt	139	139	326	326	545	545	<b>*933</b>	934	1551	1551	$\hat{\phantom{x}}2564$	2565
fe_sphere	386	386	768	768	1156	1156	1714	1714	2488	2488	3543	3543
cti	334	334	954	954	1788	1788	2793	2793	4046	4046	5629	5629
memplus	<b>*5499</b>	5513	<b>*9442</b>	9448	$\hat{\phantom{x}}11710$	11712	$\hat{\phantom{x}}12893$	12895	$\hat{\phantom{x}}13947$	13953	$\hat{\phantom{x}}16188$	16223
cs4	369	369	932	932	1440	1440	2075	2075	<b>*2907</b>	2928	$\hat{\phantom{x}}4025$	4027
bcstkt30	6394	6394	16651	16651	34846	34846	$\hat{\phantom{x}}70407$	70408	113336	113336	<b>*171148</b>	171153
bcstkt31	2762	2762	7351	7351	<b>*13280</b>	13283	<b>*23857</b>	23869	<b>*37143</b>	37158	<b>*57354</b>	57402
fe_pwt	340	340	705	705	1447	1447	2830	2830	<b>*5574</b>	5575	$\hat{\phantom{x}}8177$	8180
bcstkt32	4667	4667	9311	9311	$\hat{\phantom{x}}20008$	20009	$\hat{\phantom{x}}36249$	36250	<b>*60013</b>	60038	<b>*90778</b>	90895
fe_body	262	262	599	599	1033	1033	<b>*1722</b>	1736	$\hat{\phantom{x}}2797$	2846	<b>*4728</b>	4730
t60k	79	79	209	209	456	456	$\hat{\phantom{x}}812$	813	1323	1323	$\hat{\phantom{x}}2074$	2077
wing	789	789	1623	1623	2504	2504	$\hat{\phantom{x}}3870$	3876	$\hat{\phantom{x}}5592$	5594	$\hat{\phantom{x}}7622$	7625
brack2	731	731	3084	3084	7140	7140	11570	11570	$\hat{\phantom{x}}17382$	17387	<b>*25805</b>	25808
finan512	162	162	324	324	648	648	1296	1296	2592	2592	10560	10560
fe_tooth	3816	3816	<b>*6888</b>	6889	<b>*11414</b>	11418	$\hat{\phantom{x}}17352$	17355	<b>*24879</b>	24885	<b>*34234</b>	34240
fe_rotor	2098	2098	7222	7222	$\hat{\phantom{x}}12838$	12841	<b>*20389</b>	20391	<b>*31132</b>	31141	<b>*45677</b>	45687
598a	2398	2398	8001	8001	<b>*15921</b>	15922	<b>*25694</b>	25702	<b>*38576</b>	38581	$\hat{\phantom{x}}56094$	56097
fe_ocean	464	464	1882	1882	4188	4188	7713	7713	$\hat{\phantom{x}}12667$	12684	$\hat{\phantom{x}}20061$	20069
144	6486	6486	$\hat{\phantom{x}}15194$	15196	25273	25273	<b>*37566</b>	37571	<b>*55467</b>	55475	<b>*77391</b>	77402
wave	8677	8677	<b>*17193</b>	17198	<b>*29188</b>	29198	<b>*42639</b>	42646	<b>*61100</b>	61108	$\hat{\phantom{x}}83987$	83994
m14b	3836	3836	<b>*13061</b>	13062	<b>*25834</b>	25838	<b>*42161</b>	42172	<b>*65469</b>	65529	$\hat{\phantom{x}}96446$	96452
auto	$\hat{\phantom{x}}10101$	10103	<b>*27092</b>	27094	<b>*45991</b>	46014	$\hat{\phantom{x}}77391$	77418	<b>*121911</b>	121944	$\hat{\phantom{x}}172966$	172973

■ **Table 5** Improvement of existing partitions from the Walshaw benchmark with  $\epsilon = 1\%$  using our ILP approach. In each  $k$ -column the results computed by our approach are on the left and the current Walshaw cuts are on the right. Results achieved by  $\text{Gain}_{\rho=-1}$  are marked with  $\hat{\phantom{x}}$  and results achieved by  $\text{Gain}_{\rho=-2}$  are marked with  $*$ .

Graph / k	2		4		8		16		32		64	
add20	585	585	1147	1147	$*$ $\hat{1680}$	1681	2040	2040	2361	2361	2949	2949
data	188	188	376	376	656	656	1121	1121	1799	1799	2839	2839
3elt	89	89	199	199	340	340	568	568	953	953	1532	1532
uk	19	19	40	40	80	80	142	142	246	246	408	408
add32	10	10	33	33	66	66	117	117	212	212	485	485
bcsstk33	10097	10097	21338	21338	34175	34175	54505	54505	77195	77195	106902	106902
whitaker3	126	126	380	380	654	654	1083	1083	1664	1664	2480	2480
crack	183	183	362	362	676	676	1081	1081	1669	1669	2523	2523
wing_nodal	1695	1695	3559	3559	5401	5401	8302	8302	$*$ <b>11731</b>	11733	$*$ $\hat{15734}$	15736
fe_4elt2	130	130	349	349	603	603	1000	1000	1608	1608	$\hat{2470}$	2472
vibrobox	10310	10310	18943	18943	24422	24422	$*$ $\hat{31710}$	31712	$*$ <b>39396</b>	39400	$*$ <b>46529</b>	46541
bcsstk29	2818	2818	8029	8029	13891	13891	21694	21694	34606	34606	$*$ $\hat{54950}$	54951
4elt	138	138	320	320	532	532	927	927	1535	1535	2546	2546
fe_sphere	386	386	766	766	1152	1152	1708	1708	2479	2479	3534	3534
cti	318	318	944	944	1746	1746	2759	2759	3993	3993	5594	5594
memplus	$*$ <b>5452</b>	5457	9385	9385	11672	11672	12873	12873	$\hat{13931}$	13933	$\hat{16091}$	16110
cs4	366	366	925	925	1434	1434	2061	2061	2903	2903	$\hat{3981}$	3982
bcsstk30	6335	6335	16583	16583	34565	34565	69912	69912	112365	112365	170059	170059
bcsstk31	2699	2699	7272	7272	$*$ $\hat{13134}$	13137	$*$ <b>23333</b>	23339	$*$ <b>37057</b>	37061	$*$ <b>57000</b>	57025
fe_pwt	340	340	704	704	1432	1432	2797	2797	5514	5514	$\hat{8128}$	8130
bcsstk32	4667	4667	9180	9180	$*$ <b>19612</b>	19624	35617	35617	$*$ <b>59501</b>	59504	$*$ <b>89893</b>	89905
fe_body	262	262	598	598	1023	1023	1714	1714	$\hat{2748}$	2756	$*$ $\hat{4664}$	4674
t60k	75	75	208	208	454	454	805	805	1313	1313	2062	2062
wing	784	784	1610	1610	2474	2474	3857	3857	$\hat{5576}$	5577	$\hat{7585}$	7586
brack2	708	708	3013	3013	7029	7029	11492	11492	$*$ <b>17120</b>	17128	$\hat{25604}$	25607
finan512	162	162	324	324	648	648	1296	1296	2592	2592	10560	10560
fe_tooth	3814	3814	$*$ <b>6843</b>	6844	11358	11358	$*$ $\hat{17264}$	17265	$*$ <b>24799</b>	24804	$\hat{34159}$	34170
fe_rotor	2031	2031	7158	7158	12616	12616	$\hat{20146}$	20152	$*$ <b>30975</b>	30982	$*$ <b>45304</b>	45321
598a	2388	2388	7948	7948	15831	15831	$*$ <b>25620</b>	25624	$\hat{38410}$	38422	$*$ <b>55867</b>	55882
fe_ocean	$\hat{385}$	387	1813	1813	$*$ <b>4060</b>	4063	7616	7616	$\hat{12523}$	12524	$*$ <b>19851</b>	19852
144	$*$ <b>6476</b>	6478	15140	15140	$*$ <b>25225</b>	25232	$*$ <b>37341</b>	37347	$*$ <b>55258</b>	55277	$*$ <b>76964</b>	76980
wave	$*$ $\hat{8656}$	8657	$\hat{16745}$	16747	$*$ <b>28749</b>	28758	$*$ <b>42349</b>	42354	$*$ <b>60617</b>	60625	$\hat{83451}$	83466
m14b	3826	3826	12973	12973	$*$ $\hat{25626}$	25627	$*$ <b>42067</b>	42080	$*$ <b>64684</b>	64697	$\hat{96145}$	96169
auto	9949	9949	$*$ <b>26611</b>	26614	$*$ <b>45424</b>	45429	$*$ <b>76533</b>	76539	$*$ <b>120470</b>	120489	$\hat{171866}$	171880

■ **Table 6** Improvement of existing partitions from the Walshaw benchmark with  $\epsilon = 3\%$  using our ILP approach. In each  $k$ -column the results computed by our approach are on the left and the current Walshaw cuts are on the right. Results achieved by  $\text{Gain}_{\rho=-1}$  are marked with  $\hat{\phantom{x}}$  and results achieved by  $\text{Gain}_{\rho=-2}$  are marked with  $*$ .

Graph / k	2		4		8		16		32		64	
add20	560	560	1134	1134	1673	1673	2030	2030	2346	2346	2920	2920
data	185	185	369	369	638	638	1088	1088	1768	1768	<b>*2781</b>	2783
3elt	87	87	198	198	334	334	561	561	944	944	1512	1512
uk	18	18	39	39	78	78	139	139	240	240	397	397
add32	10	10	33	33	66	66	117	117	212	212	476	476
bcsstk33	10064	10064	20762	20762	34065	34065	54354	54354	76749	76749	<b>*105737</b>	105742
whitaker3	126	126	378	378	649	649	1073	1073	1647	1647	<b>*2456</b>	2459
crack	182	182	360	360	671	671	1070	1070	1655	1655	<b>*^2487</b>	2489
wing_nodal	1678	1678	3534	3534	5360	5360	8244	8244	<b>*11630</b>	11632	<b>*^15612</b>	15613
fe_4elt2	130	130	341	341	595	595	990	990	1593	1593	<b>^2431</b>	2435
vibrobox	10310	10310	18736	18736	24153	24153	<b>*^31440</b>	31443	<b>*39197</b>	39201	<b>*46231</b>	46235
bcsstk29	2818	2818	7971	7971	13710	13710	21258	21258	33807	33807	54382	54382
4elt	137	137	319	319	522	522	901	901	1519	1519	2512	2512
fe_sphere	384	384	764	764	1152	1152	1696	1696	2459	2459	<b>*^3503</b>	3505
cti	318	318	916	916	1714	1714	2727	2727	3941	3941	<b>*5522</b>	5524
memplus	<b>*^5352</b>	5353	9309	9309	<b>*^11584</b>	11586	12834	12834	<b>*13887</b>	13895	<b>*15950</b>	15953
cs4	360	360	917	917	<b>*^1423</b>	1424	2043	2043	<b>*2884</b>	2885	<b>^3979</b>	3980
bcsstk30	6251	6251	16372	16372	34137	34137	69357	69357	110334	110334	<b>*168271</b>	168274
bcsstk31	2676	2676	7148	7148	12962	12962	<b>*22949</b>	22956	<b>*36567</b>	36587	<b>*56025</b>	56038
fe_pwt	340	340	700	700	1410	1410	2754	2754	5403	5403	8036	8036
bcsstk32	4667	4667	8725	8725	19485	19485	<b>*^34869</b>	34875	<b>^58739</b>	58740	<b>*89478</b>	89479
fe_body	262	262	598	598	1016	1016	1693	1693	<b>*^2708</b>	2709	<b>*^4522</b>	4523
t60k	71	71	203	203	449	449	792	792	1302	1302	<b>*^2034</b>	2036
wing	773	773	1593	1593	2451	2451	<b>^3783</b>	3784	5559	5559	7560	7560
brack2	684	684	2834	2834	6778	6778	<b>*11253</b>	11256	<b>*^16981</b>	16982	<b>*^25362</b>	25363
finan512	162	162	324	324	648	648	1296	1296	2592	2592	10560	10560
fe_tooth	3788	3788	6756	6756	11241	11241	<b>*17107</b>	17108	<b>*24623</b>	24625	<b>*33779</b>	33795
fe_rotor	1959	1959	<b>*^7049</b>	7050	12445	12445	<b>*19863</b>	19867	<b>*30579</b>	30587	<b>*44811</b>	44822
598a	2367	2367	7816	7816	15613	15613	<b>*^25379</b>	25380	<b>*38093</b>	38105	<b>*55358</b>	55364
fe_ocean	311	311	1693	1693	3920	3920	7405	7405	<b>^12283</b>	12288	19518	19518
144	<b>*^6430</b>	6432	15064	15064	<b>*24901</b>	24905	<b>*^36999</b>	37003	<b>*54800</b>	54806	<b>*76548</b>	76557
wave	8591	8591	<b>^16633</b>	16638	28494	28494	42139	42139	<b>*60334</b>	60356	<b>*82809</b>	82811
m14b	3823	3823	12948	12948	25390	25390	41778	41778	<b>^64354</b>	64364	<b>*^95575</b>	95587
auto	9673	9673	25789	25789	<b>*^44724</b>	44732	<b>*^75665</b>	75679	<b>^119131</b>	119132	<b>^170295</b>	170314

■ **Table 7** Improvement of existing partitions from the Walshaw benchmark with  $\epsilon = 5\%$  using our ILP approach. In each  $k$ -column the results computed by our approach are on the left and the current Walshaw cuts are on the right. Results achieved by  $\text{Gain}_{\rho=-1}$  are marked with  $\hat{\phantom{x}}$  and results achieved by  $\text{Gain}_{\rho=-2}$  are marked with  $*$ .

Graph / k	2		4		8		16		32		64	
add20	536	536	1120	1120	1657	1657	2027	2027	2341	2341	2920	2920
data	181	181	363	363	628	628	1076	1076	1743	1743	2747	2747
3elt	87	87	197	197	329	329	557	557	930	930	1498	1498
uk	18	18	39	39	75	75	137	137	236	236	394	394
add32	10	10	33	33	63	63	117	117	212	212	476	476
bcsttk33	9914	9914	20158	20158	33908	33908	54119	54119	<b><math>\hat{76070}</math></b>	76079	<b><math>*105297</math></b>	105309
whitaker3	126	126	376	376	644	644	1068	1068	1632	1632	<b><math>*2425</math></b>	2429
crack	182	182	360	360	666	666	1063	1063	1655	1655	<b><math>*2479</math></b>	2489
wing_nodal	1668	1668	3520	3520	5339	5339	8160	8160	<b><math>*11533</math></b>	11536	<b><math>*15514</math></b>	15515
fe_4elt2	130	130	335	335	578	578	979	979	1571	1571	<b><math>*2406</math></b>	2412
vibrobox	10310	10310	18690	18690	23924	23924	<b><math>\hat{31216}</math></b>	31218	<b><math>*38823</math></b>	38826	<b><math>*45987</math></b>	45994
bcsttk29	2818	2818	7925	7925	13540	13540	20924	20924	33450	33450	53703	53703
4elt	137	137	315	315	515	515	887	887	1493	1493	<b><math>\hat{2478}</math></b>	2482
fe_sphere	384	384	762	762	1152	1152	1678	1678	2427	2427	3456	3456
cti	318	318	889	889	1684	1684	2701	2701	3904	3904	<b><math>\hat{5460}</math></b>	5462
memplus	<b><math>*\hat{5253}</math></b>	5263	<b><math>*9281</math></b>	9292	<b><math>*\hat{11540}</math></b>	11543	12799	12799	<b><math>*13857</math></b>	13867	<b><math>*15875</math></b>	15877
cs4	353	353	908	908	1420	1420	<b><math>\hat{2042}</math></b>	2043	<b><math>*2855</math></b>	2859	<b><math>*3959</math></b>	3962
bcsttk30	6251	6251	16165	16165	34068	34068	68323	68323	109368	109368	<b><math>*166787</math></b>	166790
bcsttk31	<b><math>*\hat{2660}</math></b>	2662	7065	7065	<b><math>*\hat{12823}</math></b>	12825	<b><math>*22718</math></b>	22724	<b><math>*36354</math></b>	36358	<b><math>*55250</math></b>	55258
fe_pwt	340	340	700	700	1405	1405	2737	2737	<b><math>\hat{5305}</math></b>	5306	<b><math>\hat{7956}</math></b>	7959
bcsttk32	4622	4622	8441	8441	18955	18955	34374	34374	58352	58352	<b><math>*88595</math></b>	88598
fe_body	262	262	588	588	1012	1012	1683	1683	<b><math>*\hat{2677}</math></b>	2678	<b><math>\hat{4500}</math></b>	4501
t60k	65	65	195	195	441	441	787	787	<b><math>*1289</math></b>	1291	<b><math>*\hat{2013}</math></b>	2015
wing	770	770	<b><math>*1589</math></b>	1590	2440	2440	3775	3775	<b><math>*\hat{5512}</math></b>	5513	<b><math>\hat{7529}</math></b>	7534
brack2	660	660	2731	2731	6592	6592	<b><math>*11052</math></b>	11055	16765	16765	<b><math>*25100</math></b>	25108
finan512	162	162	324	324	648	648	1296	1296	2592	2592	10560	10560
fe_tooth	3773	3773	6687	6687	<b><math>*\hat{11147}</math></b>	11151	<b><math>*16983</math></b>	16985	<b><math>\hat{24270}</math></b>	24274	<b><math>*33387</math></b>	33403
fe_rotor	1940	1940	6779	6779	<b><math>*12308</math></b>	12309	<b><math>*19677</math></b>	19680	<b><math>*30355</math></b>	30356	<b><math>*44368</math></b>	44381
598a	2336	2336	<b><math>*7722</math></b>	7724	15413	15413	25198	25198	<b><math>\hat{37632}</math></b>	37644	<b><math>*54677</math></b>	54684
fe_ocean	311	311	1686	1686	3886	3886	7338	7338	<b><math>\hat{12033}</math></b>	12034	<b><math>*\hat{19391}</math></b>	19394
144	6345	6345	<b><math>\hat{14978}</math></b>	14981	<b><math>*24174</math></b>	24179	<b><math>*\hat{36608}</math></b>	36608	<b><math>*54160</math></b>	54168	<b><math>*75753</math></b>	75777
wave	8524	8524	<b><math>*16528</math></b>	16531	28489	28489	<b><math>*\hat{42024}</math></b>	42025	<b><math>*\hat{59608}</math></b>	59611	<b><math>*81989</math></b>	82006
m14b	3802	3802	<b><math>*\hat{12858}</math></b>	12859	25126	25126	<b><math>*41097</math></b>	41098	<b><math>*63397</math></b>	63411	<b><math>\hat{94123}</math></b>	94140
auto	9450	9450	25271	25271	44206	44206	<b><math>*74266</math></b>	74272	<b><math>*118998</math></b>	119004	<b><math>\hat{169260}</math></b>	169290